Rapid Communication

A new $BaB_2Si_2O_8$:Eu^{2+}/Eu^{3+}, Tb^{3+} phosphor – Synthesis and photoluminescence properties

M.P. Saradhi [a,b,c], S. Boudin [c], U.V. Varadaraju [a,*], B. Raveau [c]

[a] Department of Chemistry, Indian Institute of Technology Madras, Chennai 600036, India
[b] Department of Chemistry, Indian Institute of Technology Hyderabad, Yeddumailaram, Hyderabad - 502205, India
[c] Laboratoire de Cristallographie et Sciences des Matériaux, ENSICAEN, Université de Caen, CNRS, 6 Bd Maréchal Juin, F-14050 Caen, France

ARTICLE INFO

ABSTRACT

In the present work, we have synthesized maleevite mineral phase $BaB_2Si_2O_8$ for the first time, which is isostructural with the pekovite mineral $SrB_2Si_2O_8$. In these europium doped host lattices, we observed the partial reduction of Eu^{3+} to Eu^{2+} at high temperature during the synthesis in air. Tb^{3+} co-doping in $MB_2Si_2O_8$:$0.01(Eu^{3+}/Eu^{2+})$ [M=Sr, Ba] improves the emission properties towards white light. The emission color varies from bluish white to greenish white under UV lamp excitation when the host cation changes from Sr to Ba.

© 2010 Elsevier Inc. All rights reserved.

1. Introduction

Study of photoluminescence of rare-earth ions in different host lattices has been of great interest from both scientific and technological point of view. Recent developments in the field of solid state lighting (SSL) have fuelled the development and demand for novel efficient inorganic luminescent materials. In this respect, europium doped materials have received special attention . Eu^{3+}, which is stable under ambient conditions, exhibits a narrow band emission, due to the forbidden f–f transitions (located 550–750 nm); on the other hand, Eu^{2+} emits in the UV-to-visible region and the emission wavelength strongly depends on the nature of the host lattice due to the participation of d orbitals (f↔d transition) [1]. The combination of the two activators, Eu^{3+} (red emission) and Eu^{2+} (blue–green emission), in a single host lattice opens the possibility to design intense white light emitting phosphors for SSL application with superior color coordinates. A great deal of work has been done on the partial reduction of Eu^{3+} and stabilization of both Eu^{3+} and Eu^{2+} in a single host lattice. The partial reduction of Eu^{3+} during the synthesis in air at high temperature was observed in several borates containing tetrahedral BO_4 groups, viz., BaB_4O_7, BaB_8O_{13}, SrB_6O_{10}, $Sr_2B_5O_9Cl$ and SrB_4O_7 [2–4]. The partial reduction of Eu^{3+}

is due to the formation of M^{2+} defects that are created due to the aliovalent substitution of Eu^{3+} for M^{2+}, according to the equation $3M^{2+} \rightarrow 2Eu^{3+} + \square_{\overline{M}}^-$. By thermal stimulation, the electrons on the vacancies would be transferred to the neighboring Eu^{3+} ions thereby reducing Eu^{3+} to Eu^{2+}. The advantage of the three-dimensional network comprised of BO_4 tetrahedral groups is that it can isolate the reduced Eu^{2+} ions by acting as a shield and resist the attack by oxygen even at high temperatures. Currently research interests are focused on finding more compounds in which Eu^{3+} could be reduced to its Eu^{2+} in air at high temperatures.

In the present study, we have synthesized and studied the optical properties of phases belonging to feldspar mineral group viz., pekovite ($SrB_2Si_2O_8$) and maleevite ($BaB_2Si_2O_8$), which are isostructural with the orthorhombic form of paracelsian ($BaAl_2Si_2O_8$) [6,7]. In these silicates, the M^{2+} [Sr, Ba] ions are embedded in the framework of corner sharing BO_4^{5-} and SiO_4^{4-} tetrahedra that form interconnected layers of 4 and 8 membered rings perpendicular to the b-axis (inset in Fig. 1a). The coordination numbers of Sr and Ba can be regarded as 9 and 10, respectively, with respect to oxygen. The existence of $BaB_2Si_2O_8$ composition was first reported by Levin and Ugrinc [8]; however, they have not isolated monophasic samples. It is of interest to synthesize this phase and study Eu^{3+} luminescence in this structure. Verstegen et al. [9], synthesized and studied the Eu^{2+} luminescence in $SrB_2Si_2O_8$. However, there is no report on the Eu^{3+} luminescence and the reduction behavior of Eu^{3+} in air in the $BaB_2Si_2O_8$ host

---

* Corresponding author. Fax: +91 44 22574202.
E-mail address: varada@iitm.ac.in (U.V. Varadaraju).

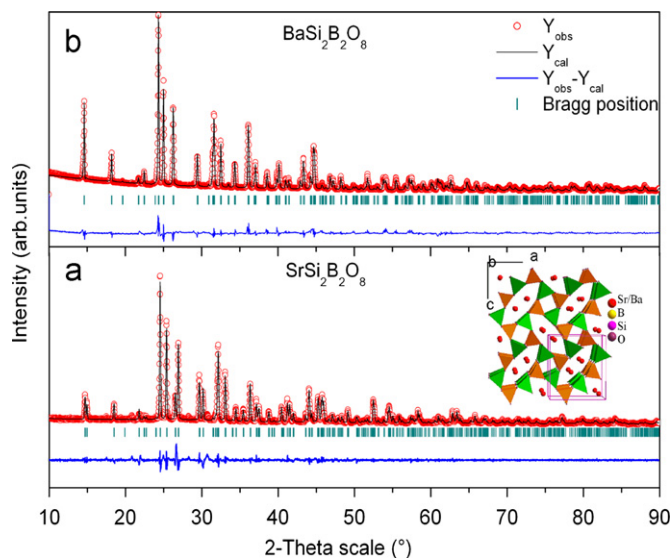**Fig. 1.** Rietveld refinement plot of powder X-ray diffraction data for (a) $SrB_2Si_2O_8$ and (b) $BaB_2Si_2O_8$.

Table 1
Crystallographic data.

Compositions	$SrB_2Si_2O_8$	$BaB_2Si_2O_8$
Space group	Pnma	Pnma
a (Å)	8.1557(4)	8.1726(2)
b (Å)	7.9224(3)	8.1837(2)
c (Å)	8.9152(3)	9.0428(2)
Cell volume (Å³)	576.0392(6)	606.0(5)
χ^2 (%)	7.80	9.51
R_b (%)	4.58	10.0
R_f (%)	4.02	6.49

450 W Xenon lamp. The CIE chromaticity coordinates were calculated by using the emission spectrum [11].

3. Results and discussion

3.1. Structural characterization

The structure refinement of powder XRD patterns of $MB_2Si_2O_8$ [Sr, Ba] was carried out based on available structural data of $SrB_2Si_2O_8$ mineral (Fig. 1). The refined lattice constants and profile factors are given in Table 1. The atomic coordinates and displacement parameters of $BaB_2Si_2O_8$ are given in Table 2. Ba^{2+} is coordinated to 10 oxygens with Ba–O bond distances of 2.876 ($\times 2$), 3.210 ($\times 2$), 2.733 ($\times 2$), 2.693 ($\times 2$), 2.918 and 2.891 Å. B^{3+} is coordinated to four oxygens with B–O bond distances of 1.540, 1.468, 1.447 and 1.404 Å. Si^{4+} is coordinated to four oxygens with Si–O bond distances of 1.706, 1.584, 1.578 and 1.555 Å. The IR spectra of $MB_2Si_2O_8$ [M=Sr, Ba] are shown in Fig. 2. As the vibrational frequencies of $[BO_4]^{5-}$ and $[SiO_4]^{4-}$ tetrahedral groups are similar, overlap of these vibrational bands is possible [12]. The IR bands around 1150 and 1110 cm^{-1} correspond to the asymmetric stretching vibration of the Si–O–Si bond [12,13]. The bands around 1020 and 860 cm^{-1} correspond to the stretching vibrations of $[BO_4]^{5-}$ tetrahedral group and the IR band at 917 cm^{-1} may be assigned to the Si–O–B linkage [13]. The IR bands at 645 and 735 cm^{-1} correspond to the bending vibrations of B–O–B bond [13]. The Si–O–B and Si–O–Si bending vibrational bands are observed around 685 and 470 cm^{-1} [14].

3.2. Diffuse reflectance spectroscopy

The diffuse reflectance spectra (DRS) of $MB_2Si_2O_8$ [M=Sr, Ba]: $0.01Eu^{3+}$ synthesized in air and $MB_2Si_2O_8$ [M=Sr, Ba]:$0.01Eu^{2+}$ synthesized in reducing atmosphere are shown in Fig. 3. Two strong and broad absorption bands around ~255, ~365 nm for $SrB_2Si_2O_8$ and ~260, ~325 nm for $BaB_2Si_2O_8$ observed for all the compositions. The bands observed in the case of $MB_2Si_2O_8$ [M=Sr, Ba]:$0.01Eu^{3+}$ phases synthesized in air are uncharacteristic of Eu^{3+}. Instead, the bands corroborate well with those of the Eu^{2+} doped phases. These bands can be ascribed to the $4f^7 \rightarrow 4f^65d^1$ electronic transitions of Eu^{2+} [1]. Thus, the DRS indicate the possible existence of Eu^{2+} in phases synthesized in air. These bands are absent in the DRS spectra of the parent phases (unsubstituted $MB_2Si_2O_8$ [M=Sr, Ba]).

3.3. Photoluminescence studies (PL)

The PL excitation and emission spectra of $MB_2Si_2O_8$ [M=Sr, Ba]:$0.01Eu^{3+}$ prepared in air are shown in Fig. 4. The spectra consist of a broad emission band in the blue region peaking at 435 and 405 nm for $SrB_2Si_2O_8$ and $BaB_2Si_2O_8$, respectively, and a series of narrow emission lines from 570 to 620 nm in the red region of

lattice. In the present study, we have synthesized monophasic $BaB_2Si_2O_8$, for the first time, and studied the optical properties of Eu^{3+}/Eu^{2+} and Tb^{3+} activated $MB_2Si_2O_8$ [M=Sr, Ba] phases. We demonstrate the partial reduction of Eu^{3+} to Eu^{2+} in air in $MB_2Si_2O_8$ [M=Sr, Ba] host lattices. While this work is underway we come across a report on reduction of Eu^{3+} in air in $SrB_2Si_2O_8$ [5]. We have shown that the co-doping with Tb^{3+} in $MB_2Si_2O_8$ [M=Sr, Ba]:Eu^{3+}/Eu^{2+} [M=Sr, Ba], improves the luminescence properties towards the generation of white light.

2. Experimental

2.1. Synthesis

The undoped and Eu^{3+} doped compounds in the present study were synthesized by high temperature solid state reaction method. The starting materials used were high pure $SrCO_3$ (Cerac, 99.99%), $BaCO_3$ (Alfa Aesar, 99.99%), SiO_2 (Alfa Aesar, 99.9%), H_3BO_3 (Alfa Aesar, 99.99%), Eu_2O_3 (Indian Rare Earths, 99.9%), Tb_4O_7 (Indian Rare Earths, 99.9%). The synthesis of $SrB_2Si_2O_8$ was carried out according to the procedure reported earlier [9]. Single phase $BaB_2Si_2O_8$ was obtained with 50 mol% of excess boric acid and heating at 850 °C/24 h in a platinum crucible followed by furnace cooling to RT. The $MB_2Si_2O_8$:$0.01Eu^{2+}$ [M=Sr, Ba] phases were synthesized under mild reducing atmosphere (5% H_2+95% Ar) in order to reduce $Eu^{3+} \rightarrow Eu^{2+}$.

2.2. Characterization

All the compositions were examined for phase formation by recording X-ray powder XRD pattern using philips X'pert diffractometer equipped with Cu$K\alpha$ radiation. Structure refinement was carried out using FULLPROF refinement program [10]. Diffuse reflectance spectra of samples were recorded using UV–visible spectrophotometer equipped with 150 mm integrating sphere attachment (V-560, JASCO). $BaSO_4$ was used as the reference. The FT-IR spectra were recorded at room temperature in KBr disc with a Thermo Nicolet 6700 FT-IR spectrometer. The room temperature photoluminescence spectra were recorded on powder samples using a Horiba Jobin Yvon Fluorolog-3 spectrofluorometer having

Table 2
Atomic coordinates, displacement parameters and occupancy of $BaB_2Si_2O_8$.

Atom	Wyckoff position	x	y	z	Biso (Å^2)	Occupancy
Ba	4c	0.388 (2)	0.25	0.0806 (2)	0.44 (4)	0.5
B	8d	0.278 (2)	0.0874 (5)	0.4075 (4)	0.50	1.0
Si	8d	0.0814 (7)	0.9296 (5)	0.1916 (5)	0.63 (11)	1.0
O1	8d	0.2176	0.9428	0.0675	0.27 (2)	1.0
O2	8d	0.1481 (13)	0.9656 (10)	0.3521 (9)	0.27 (2)	1.0
O3	8d	0.4313 (9)	0.0728 (9)	0.3285 (9)	0.27 (2)	1.0
O4	4c	0.5240 (4)	0.75	0.3302 (5)	0.27 (2)	0.5
O5	4c	0.2381 (4)	0.25	0.3735 (4)	0.27 (2)	0.5
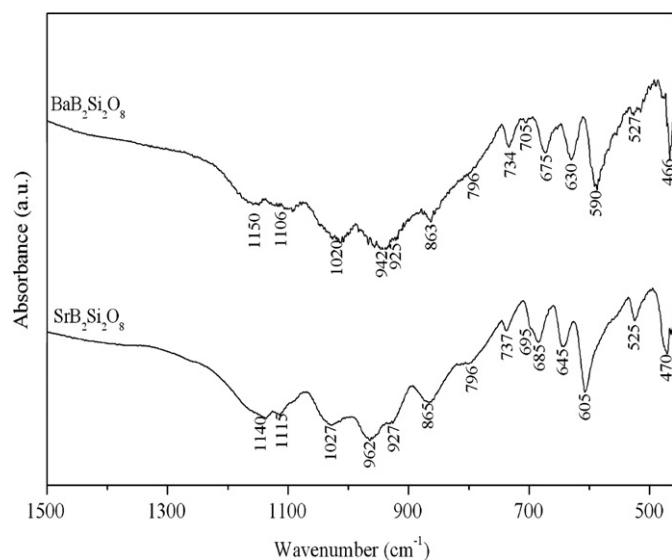
Fig. 2. FT-IR spectra of $MB_2Si_2O_8$: [M=Sr, Ba].
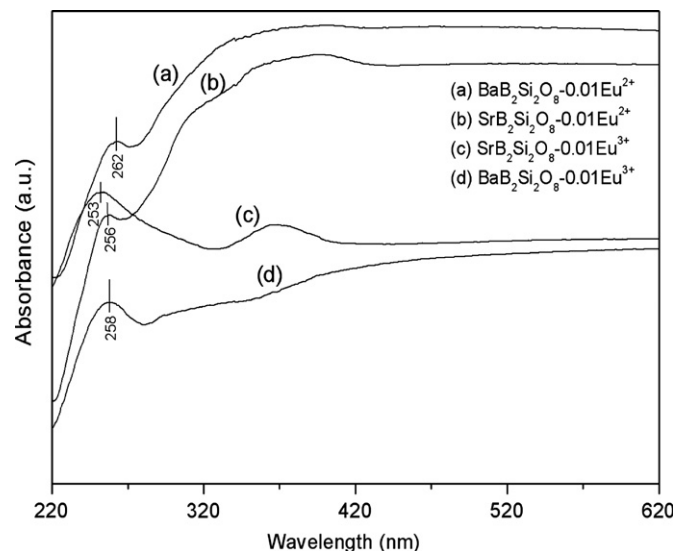
Fig. 3. UV–visible diffuse reflectance spectrum of $MB_2Si_2O_8$ [M=Sr, Ba]: 0.01Eu^{3+} synthesized in air and $MB_2Si_2O_8$ [M=Sr, Ba]: 0.01Eu^{2+} synthesized in reducing atmosphere.

Fig. 4. Photoluminescent excitation and emission spectra of $MB_2Si_2O_8$ [M=Sr, Ba]: 0.01Eu^{3+}, synthesized in air.

the visible spectrum (Fig. 4(**II**)). As is well known, the Eu^{2+} ion generally shows broad band character with $4f^n \leftrightarrow 4f^{n-1}5d^1$ transition and Eu^{3+} ion exhibits characteristic emission lines around 580 ($^5D_0 \rightarrow {}^7F_0$), 590 ($^5D_0 \rightarrow {}^7F_1$) and 615 nm ($^5D_0 \rightarrow {}^7F_2$). In the present study, the bands at 578, 591 and 611 nm indicate the
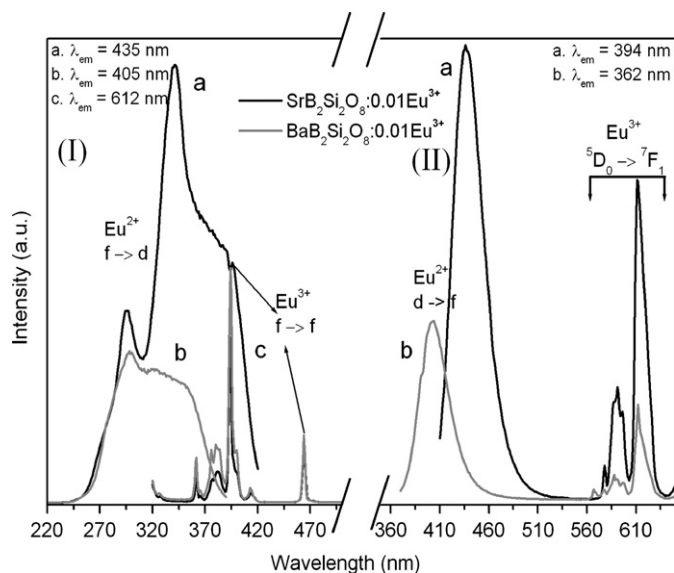
presence of Eu^{3+} in the lattice. The bands due to both electric (591 nm) and magnetic (611 nm) dipole transitions in the emission spectra confirm that the site occupied by Eu^{3+} is non–centrosymmetric. It is evident from the calculated bond distances that Ba^{2+} is presents in 10 coordinated distorted polyhedral of oxide ions.

Broad excitation and emission bands in PL spectra of $MB_2Si_2O_8$ [M=Sr, Ba]:0.01Eu^{3+} phases synthesized in air must be due to Eu^{2+} in the lattice. In order to confirm this, we synthesized Eu^{2+} activated phases $MB_2Si_2O_8$ [M=Sr, Ba]:0.01Eu^{2+} under reducing atmosphere (5%H$_2$+95%N$_2$) and compared the PL characteristics. Fig. 5 shows the PL spectra of Eu^{2+} activated $MB_2Si_2O_8$ [M=Sr, Ba]. Indeed, the broad bands at 435 and 405 nm (for the Sr and Ba analogs, respectively) are faithfully reproduced. Therefore it can be concluded that Eu^{3+} is partially reduced to Eu^{2+} in air at high temperature in borosilicate lattice $MB_2Si_2O_8$ [M=Sr, Ba]. A discussion on the position of the Eu^{2+} emission bands in the Sr and Ba analogs is in order. It is well-known that the position of the Eu^{2+} emission band is strongly dependent on the host, since the optical transition involves $4f^7 \rightarrow 4f^65d^1$. In an isostructural series of compounds consisting of alkaline earth ions doped with Eu^{2+}, crystal field splitting of the 5d levels of Eu^{2+} decreases with increasing size of the alkaline earth ion [15]. As a result, the position of the Eu^{2+} emission band shifts to shorter wavelength when the ionic radius of the cation increases, i.e., in the order Ca < Sr < Ba [15]. The observed emission bands are at 435 and 405 nm for SrB$_2$Si$_2$O$_8$ and BaB$_2$Si$_2$O$_8$ phases, respectively, following the order Sr < Ba.
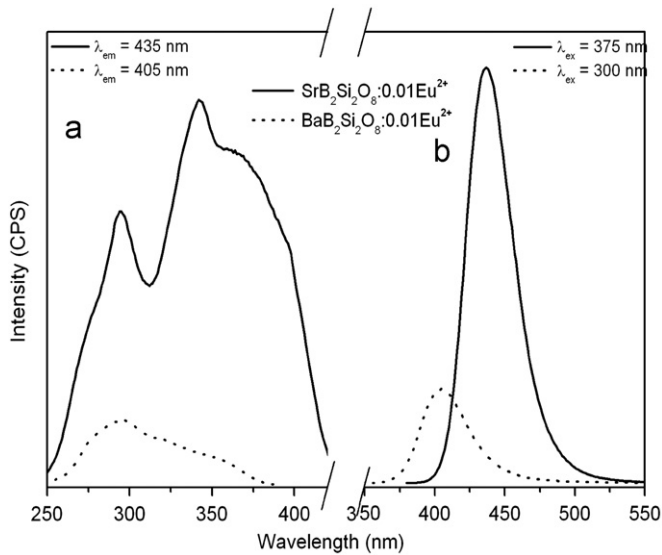
Fig. 5. Photoluminescent excitation and emission spectra of $MB_2Si_2O_8$ [M=Sr, Ba]: $0.01Eu^{2+}$ synthesized under reducing atmosphere.
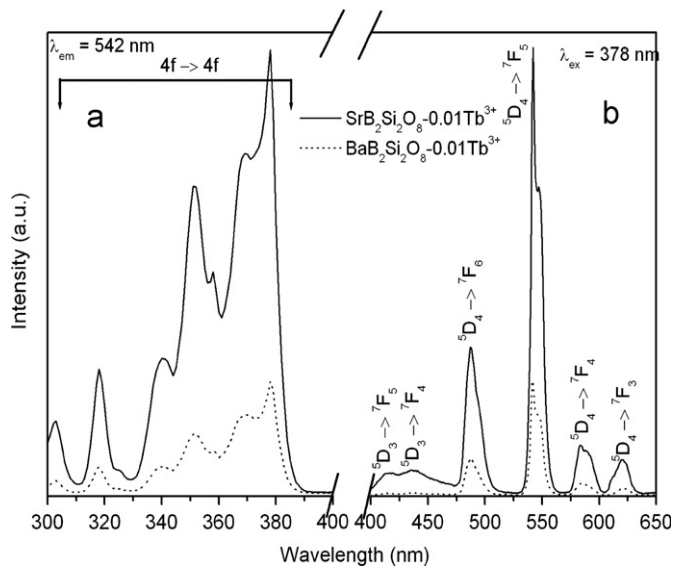

Fig. 6. Photoluminescent excitation and emission spectra of $MB_2Si_2O_8$ [M=Sr, Ba]: $0.01Tb^{3+}$, synthesized in air.

Su and coworkers have studied, systematically, the reduction process of Eu^{3+} to Eu^{2+}, when the samples were prepared in air at high temperature and proposed a charge compensation model in order to explain the abnormal reduction [16–18]. The basic requirements for a host lattice in order to affect the reduction of $Eu^{3+} \rightarrow Eu^{2+}$ in air at high temperature are the following: (1) the doped rare earth ion should replace cations with lower valences in the host, such as alkaline earth ions; (2) no other reducible ions should be present in the host; (3) the radius of the cation substituted by Eu^{2+} should be similar to that of Eu^{2+}; (4) the host compound should exhibit an appropriate crystal structure, i.e., a rigid three-dimensional network of MO_4 [M=B, Si, Al, P and S] tetrahedra is necessary to stabilize the divalent rare earth ions at high temperature in non-reducing atmosphere. The presently studied phases satisfy all the above criteria; hence, facile reduction of Eu^{3+} to Eu^{2+} (by the synthesis of the phases in air) could be affected.

Fig. 6 shows PL spectra of Tb^{3+} doped $MB_2Si_2O_8$ [M=Sr, Ba] phases. The excitation spectra exhibit a series of narrow bands in the range of 300–400 nm, which are assigned to the transitions between the energy levels of $4f^8$ configuration of Tb^{3+} ion (Fig. 6**a**) [19]. The PL emission of Tb^{3+} originates from $^5D_3 \rightarrow {}^7F_j / {}^5D_4 \rightarrow {}^7F_j$ (j=1–6) levels. The observed blue emission bands below 480 nm are due to the $^5D_3 \rightarrow {}^7F_j$ (j=5 and 4) transitions which are usually present at low concentration of Tb^{3+}. The intense emission bands in the green region at 488, 542, 585 and 620 nm are due to $^5D_4 \rightarrow {}^7F_j$ (j=6, 5, 4 and 3) transitions (Fig. 6**b**) [19,20]. In order to have a full-color-emitting phosphor that emits in the whole of visible region (blue, green and red), which is required for solid state lighting application, we have co-doped Tb^{3+} in $MB_2Si_2O_8$ [M=Sr, Ba]:$0.01(Eu^{3+}/Eu^{2+})$. The most notable feature from Figs. 4(I), 5a and 6a, is that by using selective excitation wavelengths, it is possible to excite all the activators in order to obtain emission from Tb^{3+} and Eu^{3+}/Eu^{2+}. The PL emission spectra of Tb^{3+} co-doped $MB_2Si_2O_8$:$0.01Eu^{3+}/Eu^{2+}$ synthesized in air are shown in Fig. 7. The spectra contain emission bands due to Eu^{2+}, Eu^{3+} and Tb^{3+} covering the entire visible spectral region from 350 to 650 nm. The calculated chromaticity coordinates of $MB_2Si_2O_8$ activated with Eu^{3+} and Tb^{3+} are given in Table 3. The chromaticity coordinates of rare earth doped $MB_2Si_2O_8$ phases vary significantly with respect to the doping and are approaching white region. The composition $SrB_2Si_2O_8$:$0.01(Eu^{3+}/Eu^{2+})$, $0.01Tb^{3+}$ shows bluish white emission and the composition $BaB_2Si_2O_8$:$0.01(Eu^{3+}/Eu^{2+})$, $0.01Tb^{3+}$ shows greenish white emission under UV lamp excitation.
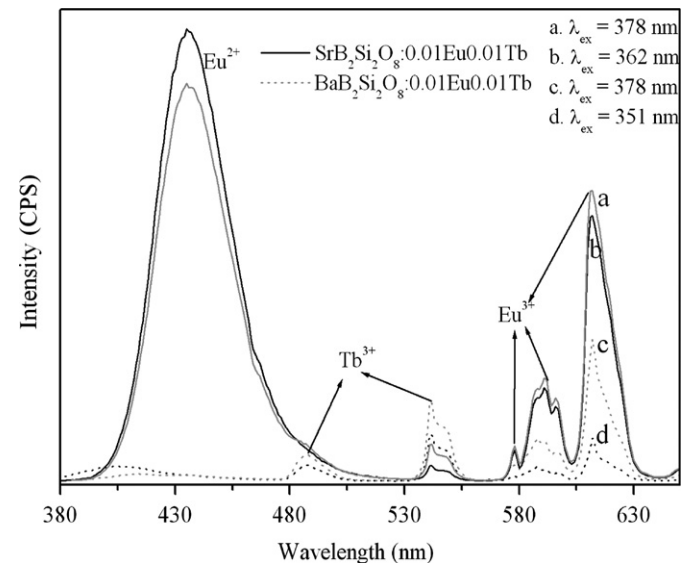

Fig. 7. Photoluminescent emission spectra of $MB_2Si_2O_8$ [M=Sr, Ba]: $0.01Eu^{3+}/Eu^{2+}$, $0.01Tb^{3+}$ synthesized in air.

Table 3
CIE Chromaticity coordinates of Eu^{3+}/Eu^{2+} and Tb^{3+} activated $SrB_2Si_2O_8$ and $BaB_2Si_2O_8$ phosphors.

Composition	Chromaticity coordinates	
	x	y
$SrB_2Si_2O_8$:$0.01Eu^{2+}$	0.1544	0.0313
$SrB_2Si_2O_8$:$0.01(Eu^{2+}/Eu^{3+})$	0.1795	0.0429
$SrB_2Si_2O_8$:$0.01(Eu^{2+}/Eu^{3+})$,$0.01Tb^{3+}$	0.2990	0.1346
$BaB_2Si_2O_8$:$0.01Eu^{2+}$	0.1638	0.0652
$BaB_2Si_2O_8$:$0.01(Eu^{2+}/Eu^{3+})$	0.2048	0.0853
$BaB_2Si_2O_8$:$0.01(Eu^{2+}/Eu^{3+})$,$0.01Tb^{3+}$	0.3890	0.4234

4. Conclusions

In this study, we have demonstrated the possibility of doping $MB_2Si_2O_8$ [M=Sr, Ba] borosilicate host lattices by Eu^{3+} and Eu^{2+} simultaneously, leading to blue and red emission, respectively. This anomalous reduction of Eu^{3+} in air is of capital importance for the stabilization of mixed valent "Eu^{3+}/Eu^{2+}" from the point of view of possible applications. We also show that the co-doping with Tb^{3+} improves the PL properties towards white region, leading to intense bluish white emission in $SrB_2Si_2O_8$ and greenish white emission in $BaB_2Si_2O_8$ under UV lamp excitation.

References

[1] G. Blasse, B.C. Grabmaier, in: Luminescent Materials, Springer-Verlag, Berlin, Germany, 1994.
[2] Q.H. Zeng, Z.W. Pei, S.B. Wang, Q. Su, Chem. Mater. 11 (3) (1999) 605–611.
[3] Z. Pei, Q. Su, J.Y. Zhang, J. Alloys Compd. 198 (1993) 51–53.
[4] Z. Pei, Q. Zeng, Q. Su, J. Phys. Chem. Solids. 61 (2000) 9–12.
[5] Y. Wang, Z. Zhang, J. Zhang, Y. Lu, J. Solid State Chem. 182 (2009) 813–820.
[6] L.A. Pautov, A.A. Agakhanov, Can. Mineral 42 (2004) 107–119.
[7] M.W. Phillips, G.V. Gibbs, P.H. Ribbe, Am. Mineral. 59 (1974) 79–85.
[8] E.M. Levin, G.M. Ugrinc, J.Res. Nat. Bur. Standards 51 (1953) 37.
[9] J.M.P.J Verstegen, J.W. Ter Vrugt, W.L. Wanmaker, J. Inorg. Nucl. Chem. 34 (1972) 3588–3589.
[10] J., Rodriguez-Carvajal, An Introduction to the Program FullProf 2000; Laboratoire Léon Brillouin, CEA-CNRS: Saclay, France, 2001.
[11] R.W.G. Hunt, in: The Reproduction of Color in Photography, Printing & Televison, Fountain Press, London, 1987.
[12] A. Rulmont, P. Tarte, J. Mater. Sci. Lett. 6 (1987) 38–40.
[13] P. Tarte, R. Cahay, A. Rulmont, G. Werding, Spectrochim. Acta 41A (1985) 1215–1219.
[14] M.A. Villegas, J.M.F. Navarro, J. Mater. Sci. 13 (1978) 2605.
[15] G. Blasse, Phys. Status Solidi (b) 55 (1973) K131–K134.
[16] Z. Pei, Q. Zeng, Q. Su, J. Solid State Chem. 145 (1999) 212–215.
[17] M. Peng, Z. Pei, G. Hong, Q. Su, Chem. Phys. Lett. 371 (2003) 1–6.
[18] M. Peng, Z. Pei, G. Hong, Q. Su, J. Mater. Chem. 13 (2003) 1202–1205.
[19] D.J. Robbins, B. Cockayne, B. Lent, J.L. Glasper, Solid State Commun. 20 (1976) 673–676.
[20] S. Kubota, H. Yamane, M. Shimada, Chem. Mater. 14 (2002) 4015–4016.